



An advanced, comprehensive thermochemical equilibrium model of a downdraft biomass gasifier

A. Ibrahim^{*}, S. Veremieiev, P.H. Gaskell

Department of Engineering, Durham University, Durham, DH1 3LE, UK

ARTICLE INFO

Article history:

Received 13 January 2022

Received in revised form

20 April 2022

Accepted 12 May 2022

Available online 26 May 2022

Keywords:

Ammonia concentration

Biomass gasification

Methane concentration

Equivalence ratio

Gasification temperature

Thermodynamic equilibrium model

ABSTRACT

A stoichiometric model is formulated for predicting the syngas yield from the reduction zone of a downdraft biomass gasifier. It incorporates the thermodynamic equilibrium of the global gasification reaction, predicts the concentration of the minor gasification products of hydrogen sulphide and ammonia as the sulphur-based and nitrogen-based contaminants, respectively, and implements a new empirical correlation, formulated using existing pertinent experimental data, to account for the mass tar yield. The governing set of model equations is solved in a fully coupled manner, with the boudouard reaction employed to predict char output and the ammonia synthesis reaction used to predict ammonia production. The model does not require the use of correction factors and satisfactorily predicts the concentration of methane, a shortcoming that has tended to plague existing equilibrium models. The syngas composition, tar and char yields, gasification temperature, cold gas efficiency and lower heating value are obtained for various biomass feedstock with a specific ultimate analysis, for different equivalence ratios and varying moisture content. Where possible, predictions are compared with corresponding experimental data and found to be in very good agreement.

Crown Copyright © 2022 Published by Elsevier Ltd. This is an open access article under the CC BY license (<http://creativecommons.org/licenses/by/4.0/>).

1. Introduction

The adverse climate effects accompanying the continued use of fossil fuels are well known. The large quantities of CO₂ and other emissions produced, coupled with the urgent desire for a more sustainable energy sector, has prompted the need for and widespread use of dependable, affordable and cleaner alternatives. Biomass has become one such promising avenue, as its modern application is considered a very optimistic clean-energy alternative. Although biomass production is invariably accompanied by the release of CO₂, it is widely viewed as a renewable energy source and is presently the only renewable that can directly replace fossil fuels due to its abundant availability, simple storage and transportation requirements, and its synthesis of different fuels and chemicals [1].

The complicated process of gasification together with the sensitivity of product distribution to the rate of heating and

residence time in a biomass gasifier, has prompted the development of mathematical models in order to characterise and predict syngas production. Such models provide a reliable representation of the chemical and physical phenomena occurring within the gasifier and are effective at providing qualitative guidance on the influence of design, operating and feedstock parameters on overall gasifier performance. Various approaches have been used to model biomass gasification systems, namely equilibrium, kinetic, CFD and neural network alternatives, with equilibrium and kinetic versions being the most extensively implemented. Although the latter can generate arguably more reliable results, they are more complicated to implement and have received far less attention compared to their equilibrium counterpart. Kinetic models incorporate reactor kinetics and hydrodynamics, suitable for long residence times when the reaction rate is very slow at a low reaction temperature and used to estimate the gas composition and temperature profiles within a biomass gasifier [2–4].

Equilibrium models, though comparatively simpler, are found to describe the gasification process well, especially for downdraft and in particular fluidised bed gasifiers which operate at close to equilibrium conditions. Although thermodynamic equilibrium cannot be reached within a gasifier, this assumption provides a reasonable prediction of the final syngas composition and are often

Abbreviations: ER, Equivalence Ratio; MC, Moisture Content; LHV, Lower Heating Value; HHV, Higher Heating Value; CGE, Cold Gas Efficiency; GFE, Gibbs Free Energy.

^{*} Corresponding author.

E-mail addresses: ahmad.ibrahim@durham.ac.uk (A. Ibrahim), s.veremieiev@durham.ac.uk (S. Veremieiev), p.h.gaskell@durham.ac.uk (P.H. Gaskell).

employed as a simulation tool for processes whose duration is normally quite long with respect to the reaction time scale, or involve high gasification temperatures ($>800\text{ }^{\circ}\text{C}$). Their main advantages is that they are relatively easy to implement with fast convergence. Two types of model can be formulated: stoichiometric and non-stoichiometric. The former are based on calculating the thermodynamic equilibrium constants of an independent set of chemical reactions which can be associated with the Gibbs free energy (GFE); the latter, are based on direct minimisation of the GFE of the chemical reaction [5].

Various experimental studies have been conducted to better understand the parameters affecting gasification kinetics. Dahou et al. [6] carried out a thermogravimetric analysis of different biomass samples to investigate biomass type and char preparation influences on steam gasification. The selected samples included agricultural residues with their inorganic element compositions measured according to solid fuel standards. The char was produced from in-situ pyrolysis of the samples and results indicated that biomass type had a much larger influence on steam gasification kinetics than the conditions used to prepare the char. The same authors [7,8] reviewed the role of inorganics on char gasification reactivity and reaction kinetics, concluding that some of the inherent inorganic elements of the biomass, such as potassium, silicon and calcium, have a significant influence. Furthermore, they established the role of potassium during steam gasification and analysed the influence of potassium carbonate on pyrolysis and gasification reactions, demonstrating that K_2CO_3 increases the reaction rate both with and without contact with the biomass, and the interaction of K_2CO_3 with the biomass is decisive for the ulterior gasification. Tamasiunas et al. [9] investigated olive biomass waste for energy recovery using thermal arc plasma gasification, finding that the charcoal derived from olive pomace, generated as a waste from the olive oil industry, had great potential for syngas production (around 55% of total produced gas). Khiari et al. [10] presented a comprehensive survey of already-well-established or future potential energy applications, including gasification and combustion of biomass derived chars, showing how they can be utilised in boilers to generate heat and/or steam to produce electricity.

Through reforming and cracking, tars can be purified resulting in a higher quality of products. As such, the experimental studies and reviews mentioned above reflect an inherent flaw in most existing mathematical models which do not consider the effects of inorganic species on the biomass gasification process.

The first recognised stoichiometric equilibrium model was developed by Zainal et al. [11] and applied to various feedstock to determine the composition of the resulting syngas and the oxygen content. An identical model was developed by Mountouris et al. [12], focusing on the thermodynamic analysis of plasma gasification, involving estimation of the resulting gas composition and energy and exergy analyses. The gasification process within a fluidised bed was investigated by Prins et al. [13] in order to describe the gasification of fuels with different compositions of organic matter, adopting a quasi-equilibrium temperature approach. Subsequently, Melgar et al. [14] and Sharma [15] developed models to predict syngas composition and reaction temperature, with the latter being provided as an initial guess and calculated iteratively. The limitation of all these models is that they do not account for the production of tar and char, which are important outputs. A model adding a pyrolysis stage based on semi-empirical correlations, instead of using thermodynamic equilibrium calculations, is reported in Puig-Arnavat et al. [16] and used to estimate the formation of gas, char and volatiles, considering tar and char leaving the gasifier as a percentage of their value in the pyrolysis stage.

Subsequently, several authors [17–24] have followed a very similar modelling approach, introducing correction factors to

modify the equilibrium constants of chemical reactions in order to obtain better agreement with experimental data. The limitation of such an approach is that it is restricted to one set of input parameters since correction factors are relevant to specific operating conditions only. The equilibrium model developed by Costa et al. [25] was optimised [26] based on the work of Jarungthammachote and Dutta [17], correcting equilibrium constants through multiplication factors representing the degree of approach to equilibrium, with their value determined by solving a multi-objective optimisation problem via the genetic algorithm MOGA II. Initially guessing a gasification temperature and providing it as an operating input variable, allowed for the chronological determination of the equilibrium constants and the syngas composition.

A parametric study of hydrogen production from steam gasification was performed by Abuadala et al. [27], with unreacted char assumed to equal 5% of the biomass carbon content and tar modelled as benzene via the empirical correlation of Corella et al. [28]. Steam gasification is simulated by first varying the amount of biomass with the quantity of steam and gasifier temperature fixed, followed by changing the operating temperature while maintaining a constant amount of steam and biomass content. An identical modelling approach has been adopted by several authors [29–31] when incorporating an empirical correlation to describe the carbon fraction representing the amount of char, based on the assumption that not all the carbon participates in equilibrium reactions. The equilibrium model of Gagliano et al. [23] fixes the tar and char yields at 4.5% and 10.5%, respectively [32,33], while utilising multiplicative factors and correlations. Ferreira et al.'s [34] review article offers a detailed description of previously developed stoichiometric and non-stoichiometric thermodynamic equilibrium models for biomass gasifiers.

Some of the above models have proved effective, acceptably determining the syngas composition compared with experimental studies. However, a good number of them either fail to calculate the tar and char yields, fix them at specific values based on experimental studies, or resort to empirical correlations to determine the production of char. Furthermore, none of the equilibrium models available in the literature allow prediction of all the key gasification parameters simultaneously, including the gasification temperature and concentrations of H_2S and NH_3 , via a fully coupled system of governing equations. Additionally, most existing equilibrium models fail to explore the effects of important working parameters, such as the equivalence ratio (ER), and do not represent the influence of some of the operating input variables on H_2S and NH_3 concentrations.

In this paper, a thermodynamic equilibrium model is presented which is not inhibited by the need for correction factors and satisfactorily predicts the amount of methane concentration in the producer gas, an output whose previous prediction has posed a major flaw. The char yield is obtained via the boudouard reaction, comparing well with experimental data for char output. The tar yield is calculated using a new empirical correlation generated through an exponential best fit curve to existing experimental tar data for downdraft gasifiers; a thermodynamic equilibrium reaction describing the formation of tars within a biomass gasifier does not exist, tar being a non-equilibrium product. The model determines the gasification temperature via the energy balance through a coupled system of equations, a robust approach offering better convergence properties. Furthermore, it embodies the production of H_2S and comprises the formation of NH_3 via the ammonia synthesis reaction. The effects of both moisture content (MC) and ER on the syngas composition, tar and char yields, gasification temperature, the lower heating value (LHV) and the cold gas efficiency (CGE) are explored and the results compared with those from the literature. Finally, particular care has been taken to

ensure that everything is consistently defined to ensure reproducibility.

2. Problem formulation and method of solution

The assumptions underpinning the model are that:

1. The gasifier operates under steady state conditions;
2. The residence time is infinite;
3. Nitrogen is considered inert;
4. The process is adiabatic;
5. The contribution of char and ash to the energy balance equation is negligible;
6. The total pressure is assumed constant (i.e. $P_0 = 101,325$ Pa), however the partial pressure of the syngas components is not and is determined via their chemical equilibrium;
7. reactants are at standard temperature (i.e. $T_0 = 298.15$ K), while products are at the unknown T .
8. tar, at standard conditions, is a mixture of liquid and gas, with its thermodynamic properties taken to be those of benzene;
9. char is assumed to have the same thermodynamic properties as graphite.

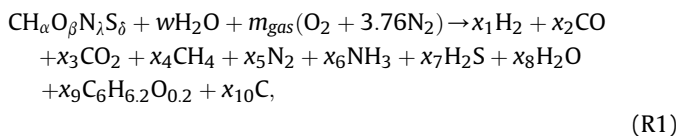
Starting from an ultimate analysis of the biomass feedstock, on a dry basis its chemical composition $\text{CH}_\alpha\text{O}_\beta\text{N}_\lambda\text{S}_\delta$ is determined via the following expressions:

$$\begin{aligned}\alpha &= \frac{y_H \times M_C}{y_C \times M_H}, & \beta &= \frac{y_O \times M_C}{y_C \times M_O}, \\ \lambda &= \frac{y_N \times M_C}{y_C \times M_N}, & \delta &= \frac{y_S \times M_C}{y_C \times M_S},\end{aligned}\quad (1)$$

where y_C, y_H, y_O, y_N and y_S are the percentage weights of C, H, O, N and S present; α, β, λ and δ are the number of atoms of the respective chemical species per one atom of carbon in the biomass, while M_C, M_H, M_O, M_N and M_S are their molar masses in kg/mol . The molar mass of biomass is expressed as:

$$M_{bm} = \frac{M_C}{y_C} \times 100\%. \quad (2)$$

The following global gasification reaction forms the basis for determining the various product species:



where w is the number of moles of H_2O per 1 mol of biomass and is calculated from the biomass MC on a wet basis as follows:

$$w = \frac{M_{bm} \times \text{MC}}{(2M_H + M_O) \times (1 - \text{MC})}, \quad (3)$$

where m_{gas} is the number of moles of gasifier input air per 1 mol of biomass; the terms x_i , for $i = 1 - 10$, indicate the number of moles of the various chemical species produced, $i = 1 - 7$ indicate components of dry producer gas which forms the gasifying medium and consists of 79% N_2 and 21% O_2 ; the number of moles of N_2 in the reactants is calculated as the amount of N_2 relative to the amount of O_2 in air. The chemical formula used to represent tar and char are $\text{C}_6\text{H}_{6.2}\text{O}_{0.2}$ [35] and C, respectively and m_{gas} is calculated as a function of ER, namely:

$$m_{gas} = \left(1 + \frac{\alpha}{4} - \frac{\beta}{2} + \frac{\lambda}{2} + \delta\right) \times \text{ER}. \quad (4)$$

For completeness, the derivation of Eq. (4) is provided in Appendix A.

The atom balance equations of C, H, O, N and S derived from the global gasification reaction, are:

$$\text{C} : x_2 + x_3 + x_4 + 6x_9 + x_{10} = 1, \quad (5)$$

$$\text{H} : 2x_1 + 4x_4 + 3x_6 + 2x_7 + 2x_8 + 6.2x_9 = \alpha + 2w, \quad (6)$$

$$\text{O} : x_2 + 2x_3 + x_8 + 0.2x_9 = \beta + w + 2m_{gas}, \quad (7)$$

$$\text{N} : 2x_5 + x_6 = \lambda + 7.52m_{gas}, \quad (8)$$

$$\text{S} : x_7 = \delta, \quad (9)$$

respectively. The specific molar heat capacity for a chemical component is determined from the following [36] empirical relationship:

$$C_{p,i}(T) = R(A_i + B_iT + C_iT^2 + D_iT^{-2}), \quad (10)$$

where subscript i denotes a particular chemical component and A_i, B_i, C_i and D_i represent the dimensionless thermodynamic empirical constants of each; their values are provided in Table 1. The enthalpy for a specific chemical component [37], while ignoring the effect of pressure for an incompressible material (i.e. solid char), is obtained from:

$$h_i(T) = h_{f,i}^\circ + \int_{T_0}^T C_{p,i}dT = J_i + R\left(A_iT + \frac{B_i}{2}T^2 + \frac{C_i}{3}T^3 - \frac{D_i}{T}\right), \quad (11)$$

where R is the ideal universal gas constant equal to 8.314 J/molK and J_i is a constant resulting from integrating the right hand side of Eq. (11) and incorporating $h_{f,i}^\circ$, namely:

$$J_i = h_{f,i}^\circ - R\left(A_iT_0 + \frac{B_iT_0^2}{2} + \frac{C_iT_0^3}{3} - \frac{D_i}{T_0}\right), \quad (12)$$

where $h_{f,i}^\circ$ is the enthalpy of formation at standard conditions for reactants and products - see Table 1 - for biomass given in Appendix A. (R1) is at a constant total pressure p_0 , therefore its enthalpy balance is equal to zero, namely:

$$\Delta H(T) = \sum_i v_i h_i(T) = 0, \quad (13)$$

where v_i is the stoichiometric number which is positive for products, $v_i = x_i$ for $i = 1 - 10$, and negative for reactants, $v_i = (-1, -w, -m_{gas}, -3.76m_{gas})$ and the summation \sum_i is repeated over all gaseous and solid components. However, note also the enthalpy of moisture is taken in liquid state while the enthalpy of char and ash is ignored.

The entropy of a chemical component at temperature T can be written [37]:

- for an incompressible material (i.e. solid char) as:

Table 1
 Constants for the molar heat capacity of chemical species and their corresponding enthalpy of formation, and GFE of formation [36].

Chemical Species	A	10 ³ B, K ⁻¹	10 ⁶ C, K ⁻²	10 ⁻⁵ D, K ²	T _{max}	h _f ^o , J/mol	g _f ^o , J/mol
Hydrogen	3.25	0.422	–	0.083	3000	–	–
Carbon Monoxide	3.38	0.557	–	–0.031	2500	–110,525	137,169
Carbon Dioxide	5.46	1.047	–	–1.157	2000	–393,509	–394,359
Methane	1.7	9.081	–2.164	–	1500	–74,520	–50,460
Nitrogen	3.28	0.593	–	0.04	2000	–	–
Ammonia	3.58	3.02	–	–0.186	1800	–46,110	–16,450
Hydrogen Sulphide	3.93	1.49	–	–0.232	2300	–20,630	–33,560
Water Vapour	3.47	1.45	–	0.121	2000	–241,818	–228,572
Tar	–2.06	39.064	–13.3	–	1500	82,930	129,665
Char	1.77	0.771	–	–0.867	2000	–	–
Nitric Oxide	3.39	0.629	–	0.014	2000	90,250	86,550
Sulphur Dioxide	5.7	0.801	–	–1.015	2000	–296,830	–300,194
Water Liquid	8.71	1.25	–0.18	–	373.2	–285,830	–237,129

$$ds_i^* = \frac{C_{p,i}}{T} dT = \frac{dh_i}{T}, \quad (14)$$

$$s_i^*(T) = s_{f,i}^o + \int_{T_0}^T \frac{C_{p,i}}{T} dT = s_{f,i}^o + \int_{T_0}^T \frac{dh_i}{T}; \quad (15)$$

where $s_{f,i}^o$ is the entropy of formation at standard conditions and

- for an ideal gas as:

$$ds_i = ds_i^* - \frac{R}{p_i} dp_i, \quad (16)$$

$$s_i(T, p_i) = s_i^*(T) - R \log\left(\frac{p_i}{p_0}\right), \quad (17)$$

where p_i is the partial pressure of a gaseous component. The GFE of a chemical component is calculated [37]:

- for an incompressible material (i.e. solid char) as:

$$d\left(\frac{g_i^*}{T}\right) = d\left(\frac{h_i}{T}\right) - ds_i^* = d\left(\frac{h_i}{T}\right) - \frac{dh_i}{T} = -\frac{h_i}{T^2} dT, \quad (18)$$

$$g_i^*(T) = g_{f,i}^o - T \int_{T_0}^T \frac{h_i(T)}{T^2} dT = J_i - RT \left(A_i \log(T) + \frac{B_i T}{2} + \frac{C_i T^2}{6} + \frac{D_i}{2T^2} + I_i \right), \quad (19)$$

where $g_{f,i}^o$ is the GFE of formation at standard conditions given in Table 1 and I_i is another integration constant determined from Eq. (19) at standard conditions, namely:

$$I_i = \frac{J_i - g_{f,i}^o}{RT_0} - \left(A_i \log(T_0) + \frac{B_i T_0}{2} + \frac{C_i T_0^2}{6} + \frac{D_i}{2T_0^2} \right); \quad (20)$$

- for an ideal gas as:

$$d\left(\frac{g_i}{T}\right) = d\left(\frac{g_i^*}{T}\right) + \frac{R}{p_i} dp_i, \quad (21)$$

$$g_i(T, p_i) = g_i^*(T) + RT \log\left(\frac{p_i}{p_0}\right). \quad (22)$$

If a reversible chemical reaction is at chemical equilibrium, then its GFE balance equals zero, and as such:

$$\begin{aligned} \Delta G(T, p) &= \sum_i \nu_i g_i(T, p_i) = \sum_i \nu_i g_i^*(T) + RT \log \prod_i \left(\frac{p_i}{p_0}\right)^{\nu_i} \\ &= \Delta G^*(T) + RT \log k(T) = 0. \end{aligned} \quad (23)$$

Accordingly, the thermodynamic equilibrium constant, $k(T)$, of the reaction is determined from Dalton's law as follows:

$$\log k(T) = \log \prod_i \left(\frac{p_i}{p_0}\right)^{\nu_i} = \log \prod_i \left(\frac{x_i}{N_{tot}}\right)^{\nu_i}, \quad (24)$$

where the multiplication \prod_i is repeated over the reactions gaseous components only. $N_{tot} = \sum_{i=1}^9 x_i$ is the number of moles of the raw producer gas at temperature T and the equilibrium constant is calculated via the standard gibbs free energy, $\Delta G^*(T)$, of a reaction:

$$\log k(T) = -\frac{\Delta G^*}{RT} = -\frac{1}{RT} \sum_i \nu_i g_i^*(T), \quad (25)$$

where the summation \sum_i is repeated over all the reactions gaseous and solid components.

Four independent equilibrium reactions are implemented to model the gasification process: the methanation, water-gas shift, boudouard and ammonia synthesis reactions:



respectively. (R2) progresses rapidly with hydrogen being reduced to form methane in the presence of carbon; (R3) increases the hydrogen concentration at the expense of carbon monoxide and describes the equilibrium between the two in the presence of water. In the absence of steam and in the presence of air as a

gasifying medium, (R4) is dominant; therefore, it is implemented in order to describe the conversion of char to carbon monoxide in the presence of carbon dioxide. As reported in Gambarotta et al. [38], ammonia is the most abundant nitrogen-based syngas contaminant and its production is accounted for via (R5) [39]. Accordingly, the equilibrium constants, k_{R2} , k_{R3} , k_{R4} and k_{R5} for the above chemical reactions are obtained from Eq. (24) as follows:

$$k_{R2}(T) = \frac{x_4 \times N_{tot}}{x_1^2}, \quad k_{R3}(T) = \frac{x_1 \times x_3}{x_2 \times x_8},$$

$$k_{R4}(T) = \frac{(x_2)^2}{x_3 \times N_{tot}}, \quad k_{R5} = \frac{x_6^2 \times N_{tot}^2}{x_5 \times x_1^3}, \quad (26)$$

and at temperature T are calculated from Eq. (25). Tar is modelled by taking its thermodynamic properties to be those of benzene. To account for tar production, a unique empirical correlation is generated in the form of an exponential best fit curve using appropriate tar data, gathered from experiments performed on downdraft biomass gasifiers [40–44] using gas chromatography and separation techniques. While corresponding data is available for other than downdraft gasifiers, it is either not provided in the preferred mass tar yield format or can be converted into the same. Mass tar yield on dry basis (% d.b.) offers a coherent dimensionless form that removes any dependence on the dimensional properties of biomass and gasifier length scales. Accordingly, the above tar data (denoted in units of g/Nm^3) was converted to mass tar yield (wt.%) as follows:

$$\text{tar content} = \frac{\text{tar yield}}{\text{syngas yield} \times 100\%},$$

where $\text{syngas yield} = \frac{N_{gas} \times V_m}{M_{bm}}, \quad (27)$

where $N_{gas} = \sum_{i=1}^7 x_i$ is the number of moles of the dry producer gas at standard temperature and $V_m = 22.4$ Litres is the volume for an ideal gas at standard temperature and pressure. This was done for all the associated ER values, obtaining the amount of tar per unit mass of biomass, thus achieving consistency in the determination of the mass tar yield between the respective experimental studies.

The resulting data points are plotted in Fig. 1. The tar yield is expressed as a function of ER only since it is the most important operating condition influencing biomass gasification, affecting both the producer gas composition and T ; since T is an output parameter its effect is not reflected in the resulting mass tar yield relationship. The effect of the other operating condition, MC, is much less significant [39,45]. Shown also is the curve fit obtained using the experimental data of [40–43] and Matlab's Curve Fitting Toolbox app; the data of [44] is shown for completeness, being clearly inappropriate for this purpose due to its uncorrelated nature. The resulting empirical relationship in equation form is given by:

$$\text{tar yield} = 0.8212 \exp(-3.281ER) \times 100\%, \quad (28)$$

with the molar tar yield, as used in the model formulation, given by:

$$x_9 = 0.8212 \exp(-3.281ER) \times \frac{M_{bm}}{M_{tar}} \quad \text{for } 0.155 \leq ER \leq 0.415, \quad (29)$$

where $M_{tar} = 6M_C + 6.2M_H + 0.2M_O$ is the molar mass of tar. The curve decreases with increasing ER, showing a low tar yield, which is to be expected since downdraft gasifiers normally produce a low tar content ($<1g/Nm^3$) [39]. Unlike previous equilibrium

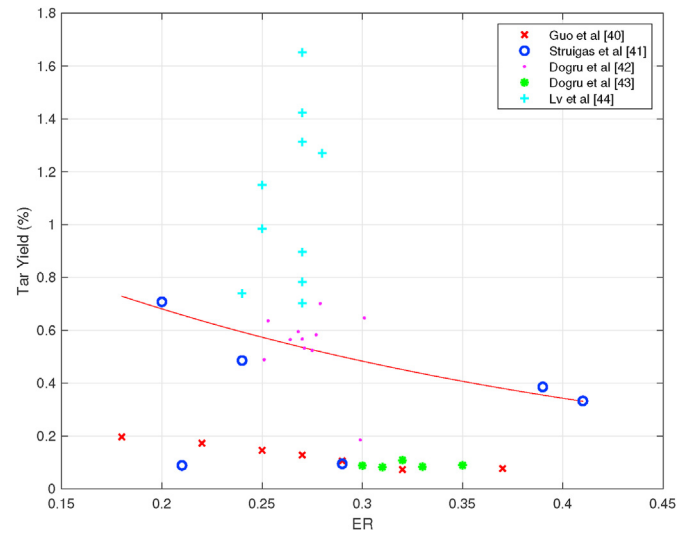


Fig. 1. Downdraft gasifier tar yield as a function of ER: showing corresponding experimental data and best-fit relationship, Eq. (28), based on the datasets [40–43].

models, such as [26,27,31], which adopted Correla et al.'s [28] correlation, generated for a fluidised bed gasifier, and that of Kirsanovs et al. [46] who failed to show how the tar model fitted with experimental data, the above curve-fit provides a reliable prediction of the tar yield as the experimental tar data was gathered from the outputs of downdraft biomass gasifiers only.

The system of Eqs. (5)–(9) as well as Eqs. (13), (26) and (29) consist of 11 equations for the 11 unknowns $x_1, x_2, x_3, x_4, x_5, x_6, x_7, x_8, x_9, x_{10}$ and T , and are solved numerically using Matlab's built-in function `fsolve` - details of its implementation are provided in Ref. [47]. For all the results generated and discussed subsequently, the 11 unknowns were assigned the same starting values namely $(x_i, i = 1 - 10, T) = (0.05, 0.06, 0.03, 0.03, 0.07, 0.05, 0.02, 0.07, 0.081, 0.091, 1000.0 K)$. One of the advantages of the current approach is determination of the gasification temperature, T , via a more robust fully coupled solver offering better convergence properties.

The molar LHV of the dry producer gas at standard temperature (MJ/mol) is given by:

$$\text{LHV}_{gas} = \frac{1}{N_{gas}} \sum_{i=1}^7 x_i \text{LHV}_i, \quad (30)$$

where LHV_i is the molar LHV of component i at standard temperature calculated from their complete combustion reactions as follows:

$$\begin{aligned} \text{LHV}_1 &= h_{f,1}^\circ - h_{f,8}^\circ, \quad \text{LHV}_2 = h_{f,2}^\circ - h_{f,3}^\circ, \quad \text{LHV}_3 = 0, \\ \text{LHV}_4 &= h_{f,4}^\circ - h_{f,3}^\circ - h_{f,8}^\circ, \quad \text{LHV}_5 = 0, \\ \text{LHV}_6 &= h_{f,6}^\circ - h_{f,5}^\circ - h_{f,8}^\circ, \quad \text{LHV}_7 = h_{f,7}^\circ - h_{f,8}^\circ - h_{f,SO_2}^\circ. \end{aligned} \quad (31)$$

The volumetric LHV of producer gas at standard temperature (MJ/mol) is given by the following:

$$\text{LHV}_{gasvol} = \frac{\text{LHV}_{gas}}{V_m}. \quad (32)$$

The CGE [48], which is the ratio of the LHV of the syngas and the LHV of the biomass feedstock, as calculated in Appendix A is given as follows:

$$CGE = \frac{LHV_{gas}}{LHV_{bm}} \times 100\% \tag{33}$$

3. Results and discussion

The chemical and physical properties of the feedstock considered, as a necessary pre-requisite of any biomass gasification study, are obtained through characterisation tests; the ultimate and proximate analysis of the feedstocks and their higher heating value (HHV) calculated via Eq. (A.11) - see Appendix A - are provided in Table 2.

3.1. Model validation

First, the producer gas composition is compared with a set of experimental data and corresponding model predictions, highlighting the satisfactory prediction of the methane concentration, with the species concentration of component *i* at standard temperature is given by:

$$\text{concentration} = \frac{x_i}{N_{gas}} \times 100\% \tag{34}$$

Next, the predicted temperature *T* is compared with experimental data, showing its influence when the operating parameters are varied. Finally, the char yield is calculated as a percentage of biomass on a dry basis (%d.b.) as follows:

$$\text{char yield} = \frac{x_{10} \times M_C}{M_{bm}} \times 100\% \tag{35}$$

and compared with existing experimental data, clearly showing the reliability of implementing the boudouard reaction.

3.1.1. Producer gas composition

The results of this section compare predicted and experimentally observed producer gas compositions for different feedstock as a function of MC and ER. The comparison is based on the main output gases forming the producer gas of a typical downdraft gasifier (i.e. H₂, CO, CO₂, CH₄ and N₂).

It can be seen from Fig. 2a and b that the predictions are in reasonably good agreement with the experimental data of Jayah

et al. [49] and Barrio et al. [50]; any differences can be attributed to the fact that the model incorporates tar, char and accounts for minor gasification products. Shown also are the corresponding solutions obtained by Ref. [23] for the same feedstocks; noting that both sets of predictions overestimate the hydrogen and underestimate the methane concentrations. Such behaviour is typical of equilibrium models which others [56,57], justify on the basis that methane produced in the low temperature zone can bypass the reaction zone and avoid reduction - see also [24]. The predicted methane concentration for rubberwood and wood pellets is found to be 1.03% and 0.78%, respectively showing that the current model is better at predicting the methane concentration when compared with experimental data whilst demonstrating a more sophisticated syngas composition, the objective of developing biomass gasifiers being to increase the amount of H₂ and CO while maintaining a relatively low amount of CO₂. For the results obtained by Ref. [23], the model was calibrated to achieve a more favourable outcome, accomplished by introducing correction factors for (R2), thus moving the reaction equilibrium towards more CH₄ and less H₂ production and for (R3), thus moving the reaction equilibrium towards more CO and less H₂ production. Nevertheless, the current model is better able to predict the concentration of CH₄, and in some cases the syngas; also comparison with the experimental data of [50] shown in Fig. 2b is better for the current model than for the equilibrium model of [23].

Fig. 3 compares the producer gas composition obtained using the current model with experimental data from Refs. [51,52]. Fig. 3a is for the case of rice husk at an ER of 0.45 and moisture free basis, showing good agreement with the data of Yoon et al. [51], especially for the case of N₂ concentration. The model leads to a slightly higher CO concentration but still aligns well with the experimental study. Fig. 3b relates to the gasification of bamboo at an ER of 0.3 and MC of 10% showing good overall agreement with the data of Dutta et al. [52]. Fig. 3c is for the gasification of neem at an ER of 0.3 and an MC of 20%, showing good agreement between the predictions and the experiments of [52].

A detailed comparison of the predicted syngas composition and those measured by Ref. [49] is provided in Table 3, from which it is clear that as the MC decreases and the ER increases, the H₂ and CO₂ concentrations decrease. Obviously, the amount of N₂ increases with increasing ER, resulting from the higher amount of air present in the system. For the same operating conditions, the syngas composition predicted by the model compares well with the corresponding measured values, but with slightly higher production

Table 2
The ultimate and proximate analysis of different biomass feedstocks.

Biomass Feedstock	Ultimate Analysis					Proximate Analysis			
	y _c (wt.%d.b.)	y _H (wt.%d.b.)	y _O (wt.%d.b.)	y _N (wt.%d.b.)	y _S (wt.%d.b.)	y _{FC} (wt.%d.b.)	y _{VM} (wt.%d.b.)	y _{ASH} (wt.%d.b.)	HHV(MJ/kg d.b.)
Rubberwood [49]	50.6	6.5	42	0.2	—	19.2	80.1	0.7	20.98
Wood pellets [50]	50.67	6.18	40.97	2	0.18	—	—	1	20.7
Rice husk [51]	33.14	5.14	37.20	0.55	0.1	20.1	60	23.85	15.81
Bamboo [52]	48.39	5.86	39.21	2.04	—	15.2	80.3	4.5	19.62
Neem [52]	45.1	6	41.5	1.7	—	12.65	81.75	5.6	18.38
Pellets [53]	46.97	5.82	39.52	0.06	0.31	—	—	0.85	19.18
Wood chips 1 [53]	49.99	5.24	41.07	0.17	0.67	—	—	0.06	19.36
Wood chips 2 [53]	48.51	5.51	36.86	0.10	0.43	—	—	0.89	19.64
Wood chips 3 [53]	46.83	5.92	39.84	0.06	0.33	—	—	0.41	19.23
Wood chips 4 [54]	49.44	6.06	43.51	—	—	—	—	1	19.87
Lignite [55]	37.80	4.93	40.394	1.625	0.141	31.03	42.07	15.11	16.37
Mixed wood chips [41]	48.77	5.85	44.52	0.05	0.01	12.8	75.8	0.8	17.3
Softwood pellets [41]	49.20	6.20	44.06	0.08	0.06	15.2	79.2	0.4	19
Rape straw pellets [41]	39.60	5.60	48.54	0.78	0.08	17.2	62.5	5.4	16.2
Poultry litter pellets [41]	43.98	5.16	31.98	4.63	0.75	15.3	63.6	13.5	16.8
Sewage sludge - sawdust pellets [41]	41.08	5.51	26.90	3.77	0.94	14.3	59.5	21.8	17.8
Forest waste [38]	53.1	6.2	36.62	1.11	0.07	—	—	2.9	19.2

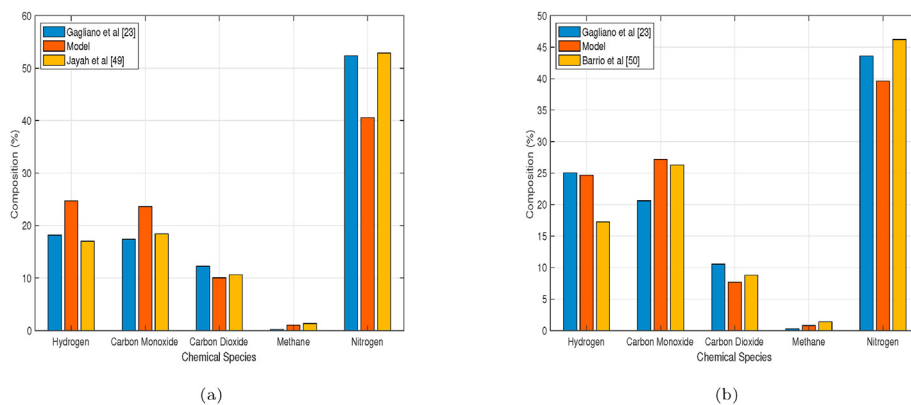


Fig. 2. Comparison between predicted ([23] and the model) and experimentally obtained [49,50], producer gas composition for (a) rubberwood (MC = 16%, ER = 0.314) and (b) wood pellets (MC = 8% and ER = 0.266).

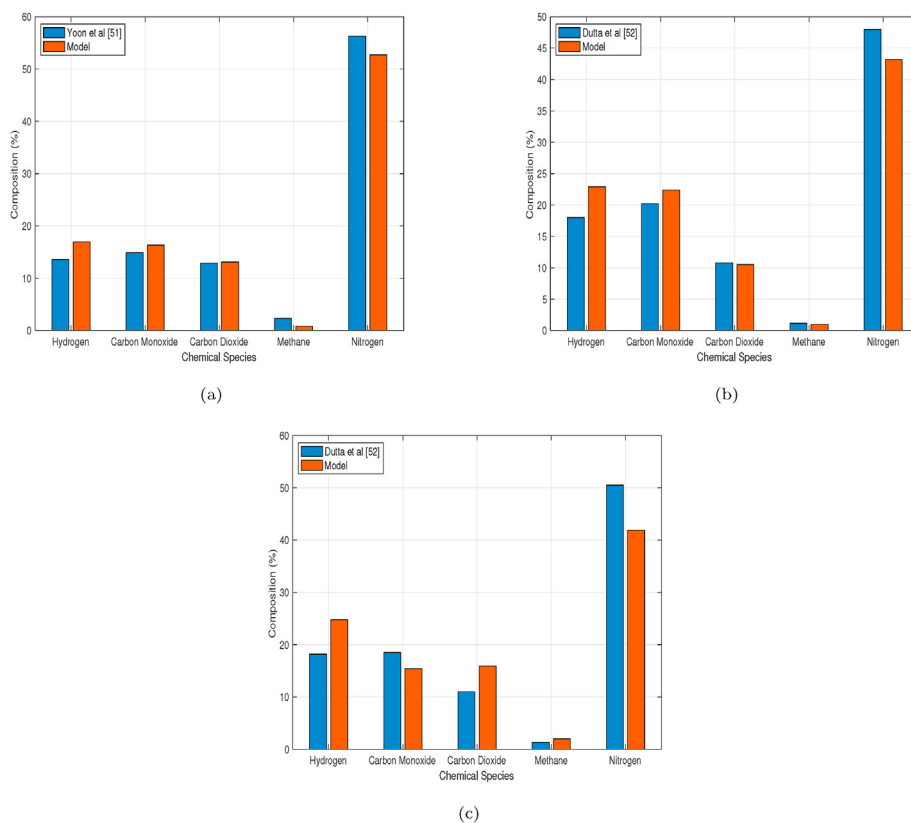


Fig. 3. Comparison of the producer gas composition obtained experimentally [51,52], and predicted by the model for (a): rice husk (MC = 0%, ER = 0.45), (b): bamboo (MC = 10%, ER = 0.3) and (c): neem (MC = 20%, ER = 0.3).

levels of H₂ and CO.

Finally, the syngas composition predicted by the model is compared with a wider range of experimental datasets performed on state-of-the-art small-scale downdraft biomass gasifiers, currently in operation [53], as shown in Fig. 4. This was achieved for the different feedstocks by evaluating the producer gas composition at the respective ER and MC for the specific technology. The predicted results are in fairly good agreement with those of the experimental studies; the differences can reasonably be attributed to the fact that there are other major operating conditions which affect the gas composition in operational downdraft gasifiers such as thermal and electrical efficiencies and gasifier design. For

equilibrium models, the ER has the biggest influence on the

Table 3
Syngas composition (%), for different operating conditions, predicted by the model and obtained experimentally [49].

	MC %	ER	H ₂	CO	CO ₂	CH ₄	N ₂
Jayah et al [49]	18.5	0.33	17.2	19.6	9.9	1.4	51.9
	16	0.35	18.3	20.2	9.7	1.1	50.7
	14.7	0.38	17.2	19.4	9.7	1.1	52.6
Prediction	18.5	0.33	24.50	22.93	10.53	1.08	40.92
	16	0.35	23.83	23.59	10.01	0.96	41.57
	14.7	0.38	22.21	26.33	7.96	0.67	42.80

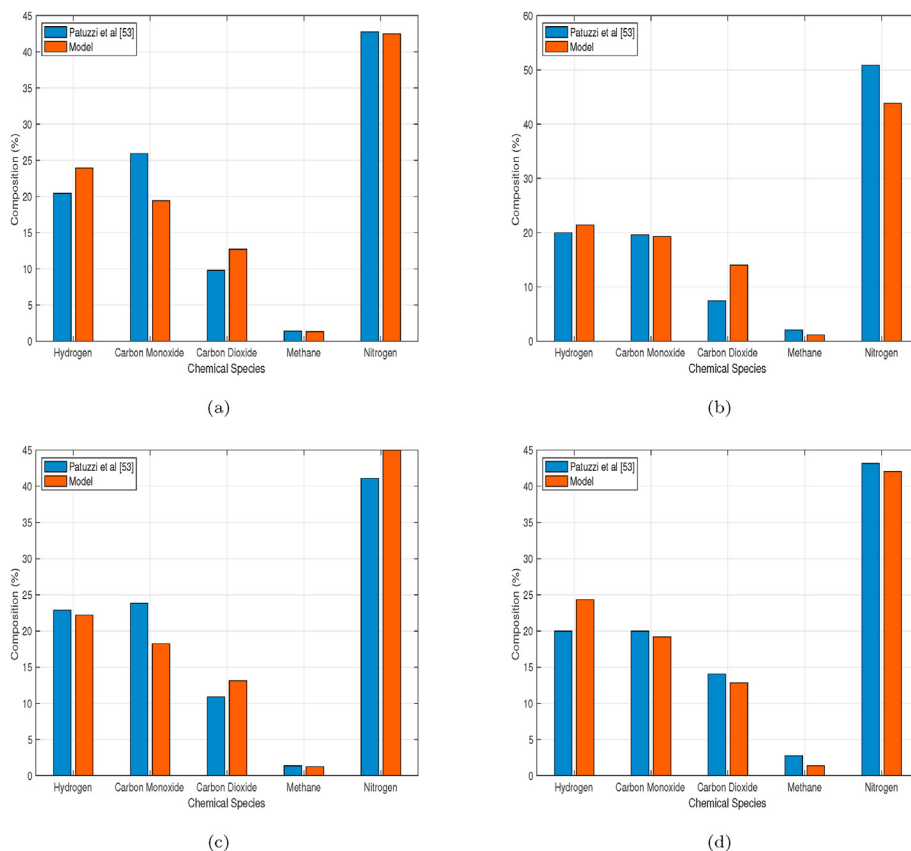


Fig. 4. Comparison between predicted and experimentally obtained [53] producer gas composition for (a): pellets (MC = 6.32%, ER = 0.26), (b): wood chips 1 (MC = 3.39%, ER = 0.25), (c): wood chips 2 (MC = 10.30%, ER = 0.29) and (d): wood chips 3 (MC = 7.65%, ER = 0.26).

producer gas composition, noting the proportional relationship between ER and N₂. The predicted CH₄ agrees well with the corresponding experimental values - especially in the case of feedstocks (a) and (c) - highlighting the uniqueness of the current model as this has never been achieved by previous equilibrium models without the introduction of empirical correction factors. As for the H₂ prediction, in some cases it is overestimated but for the obvious reasons already mentioned.

3.1.2. Gasification temperature

Fig. 5a provides a comparison of the predicted *T* against its counterpart from the experimental study of Upadhyay et al. [55]. The two profiles have the same trend with *T* increasing with

increasing ER, which is expected due to the higher amount of air present in the system, thereby enhancing the extent of the combustion reaction which ultimately increases the amount of heat released, thus facilitating *T*. A mixture of lignite - sawdust briquettes (70:30 wt%) is used as feedstock and minor differences can be attributed to the fact that in experimental studies such as [55], various other gasifier conditions affect *T*, compared with equilibrium models where only the ER and MC have a strong influence. Evidently, Fig. 5a shows a good comparison of the model's *T* with that obtained experimentally by Ref. [55].

Fig. 5b shows the influence of MC on the predicted *T* compared with that obtained experimentally by Ref. [54] at an ER of 0.25; both show a decrease in *T* with increasing MC, which is attributable to

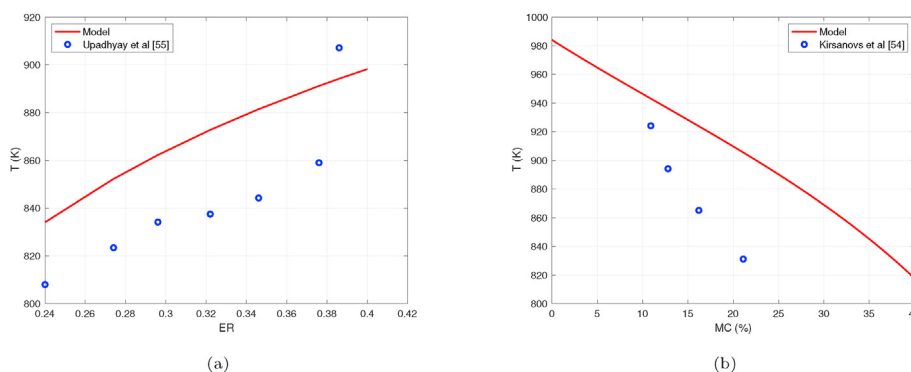


Fig. 5. Variation of *T* with ER for (a) lignite (MC = 12%) and with MC for (b) wood chips 4 (ER = 0.25).

the fact that an increase in MC in the feedstock favours endothermic behaviour which tends to decrease the reaction temperature, consequently decreasing the T [58]. There is a significant difference in T at an MC of around 21%, but good agreement between the model and the experimental investigation can be favourably argued for T between the MC range. As explained, the factors influencing T in experimental investigations constitute additional operating parameters. For example [54], demonstrates also the primary and secondary air flow, fuel supply rate as well as the thermal capacity of the gasifier, as all having an effect on T .

3.1.3. Char yield

(R4) is used to account for the char yield prediction, due to it being the more dominant reaction when using air as gasifying medium [39], rather than using an empirical correlation to describe the carbon fraction, a factor representing the amount of carbon that participates in equilibrium reactions, as utilised in previous thermodynamic equilibrium models - see for example [24,29–31]. In order to confirm the viability and reliability of implementing the boudouard reaction, the predicted char yield is compared with the results obtained from the experimental investigation of a downdraft biomass gasifier by Ref. [41] in Fig. 6 for a variety of biomass feedstock and different operating conditions. On the whole two are in comparatively good agreement. In thermodynamic equilibrium models, ER is capable of affecting main- and by-product yields significantly and normally, the char yield decreases with ER since increased ER favours enhanced bed temperature, enhancing char reactions through (R3) and (R4) and consequently a higher amount of gas is formed. As such, this would explain the extreme variation in the char yield comparison for softwood pellets as it was carried out at an ER of 0.2. For both model and experiment, the lowest char yield occurs for the gasification of mixed wood chips. For the remaining feedstocks of a more pelletised nature, the char yield increases, but varies depending on the amount of ash in the raw material, the ER and T . The amount of ash in mixed wood chips is 0.8, which is 24 times less than the amount of ash found in softwood pellets, thus explaining the extreme variation in the predicted char yield between the feedstocks.

Attention is now turned to using the model to explore the effect

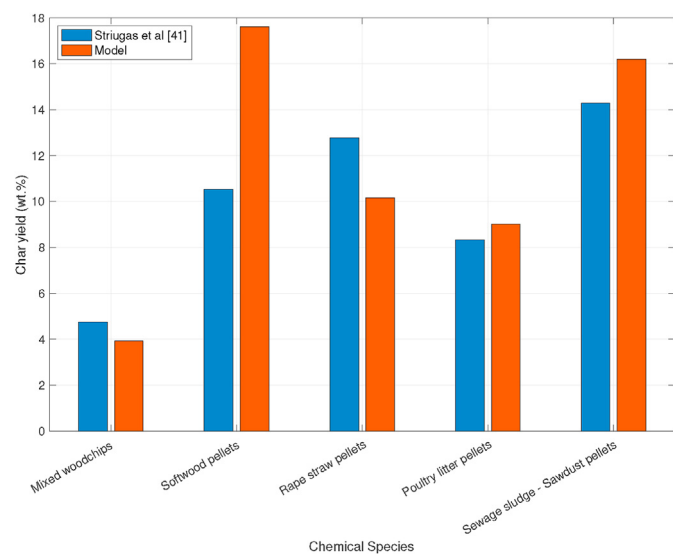


Fig. 6. Comparison of predicted char yield with that obtained experimentally by Ref. [41] for mixed wood chips (ER = 0.21), softwood pellets (ER = 0.20), rape straw pellets (ER = 0.29), poultry litter pellets (ER = 0.41) and sewage sludge - sawdust pellets (ER = 0.39).

of operating conditions such as MC and ER for rubberwood and wood pellets. This is followed by considering the case of ammonia and hydrogen sulphide concentration as components of the producer gas composition.

3.2. Effect of moisture content

MC is an essential property of biomass and an important operating parameter when developing a gasifier since it can strongly influence the conversion of biomass into energy. Increasing levels of moisture affects the self-sustainability of the combustion process, ultimately decreasing the heating value of the syngas and reducing the efficiency of the process. Furthermore, high levels of moisture reduce the oxidation temperature leading to an incomplete cracking of the hydrocarbons produced during pyrolysis. Tolerable biomass moisture level limits range from 15% to roughly 55% [5].

In Fig. 7, the effect of MC in rubberwood on the composition of the resulting producer gas is revealed. As MC increases from 0% to 40%, the percentage of CO₂ increases from around 5%–20%, while the percentage CO decreases from approximately 31%–11%. The N₂ concentration remains almost constant with increasing MC, as expected, while the CH₄ produced varies marginally from 0.5% to around 3.5%, indicating the improved prediction of CH₄ by the current equilibrium model relative to experimental studies of downdraft biomass gasifiers. The H₂ concentration increases slightly from 22% to around 26% with increasing MC in agreement with the findings of [11,23].

Fig. 8a and b consider the LHV and the CGE, for both rubberwood and wood pellets, respectively, as a function of the MC and a fixed ER of 0.326. Both decrease with increasing MC. This is anticipated considering the greater reduction in CO concentration compared to the slight increase in the H₂ concentration as the MC increases, as shown in Fig. 7 for rubberwood. In the case of the CGE, increasing MC decreases the efficiency of the gasifier as T decreases with MC resulting in a weaker production of syngas.

The corresponding variation of tar content with MC is shown in Fig. 9, that for rubberwood being slightly greater than that of wood pellets for the same operating conditions. The decrease in tar content with MC is in line with the results of [59] who studied the influence of MC on the tar characteristics of wood pellet feedstock in a downdraft gasifier using gas chromatography, mass spectrometry and gravimetric analysis to identify and analyse the tar

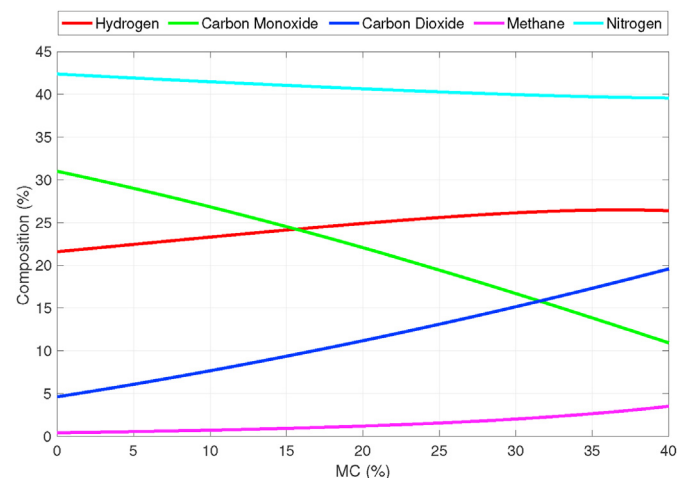


Fig. 7. Predicted variation of syngas composition with MC for rubberwood (ER = 0.326).

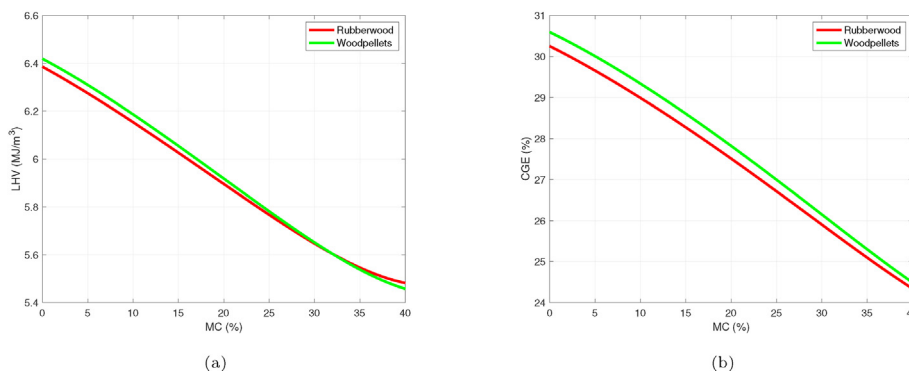


Fig. 8. Predicted variation with increasing MC for (a) LHV_{gas} and (b) CGE for rubberwood and woodpellets (ER = 0.326).

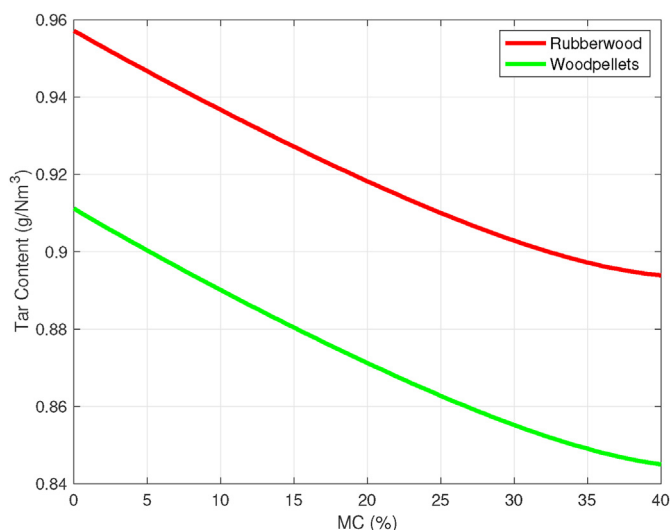


Fig. 9. Predicted variation of tar with MC for rubberwood and woodpellets (ER = 0.326).

samples.

3.3. Effect of equivalence ratio

ER is the main operating parameter influencing biomass gasification, which is considered as a fuel rich combustion when the ER is less than 1. Typical values usually range from 0.2 to 0.4, and strongly affect the gasification process as it determines the temperature of the system, oxygen availability, the syngas output and thus the gas composition and heating value in addition to the tar yield [5,39].

The influence of the ER on the syngas composition at 18.5% MC for rubberwood is shown in Fig. 10. The H_2 concentration decreases while that of CO increases with increasing ER, which is due to the fact that a higher ER will ultimately result in a higher T which facilitates the endothermic reaction (i.e. the formation of CO_2 and CO). The amount of CO_2 correspondingly decreases due to the increased T and the boudouard reaction. The CH_4 concentration is found to decrease fractionally from around 2.5%–0.75%; this is due to the fact that the higher T facilitates the rate of the water-gas shift and the boudouard reactions but decreases the rate of the methanation reaction. The decrease in H_2 concentration is in-line with the results of [55,60,61]. Finally, the N_2 concentration in the producer gas increases because the N_2 is mainly in air and at a higher ER, more air is present in the system.

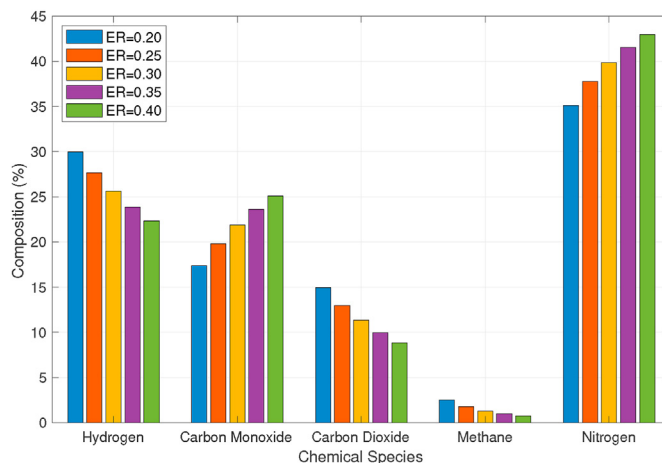


Fig. 10. Predicted variation of producer gas composition with ER for rubberwood (MC = 18.5%).

Fig. 11a explores the variation of the LHV for rubberwood with MC for different ER values. It is shown that the reduction of high heating value gases such as H_2 and CH_4 and heavier hydrocarbons, in addition to the dilution effects of N_2 , decreases the LHV of the producer gas with increasing ER. The same outcome was obtained by Cho et al. [62], who reported that increasing ER from 0.21 to 0.41 led to a reduction of LHV from 13.42 to 7.05 MJ/Nm³. The variation of CGE with MC for increasing values of ER, Fig. 11b, exhibits a similar trend to the LHV_{gas} with CGE decreasing with increasing ER. A similar result was reported by Ref. [63] with the heating value decreasing from 11.3 to 5.17 MJ/Nm³ for an increase of ER from 0.2 to 0.45. At a low ER (≤ 0.25), the low quality syngas results in an increase followed by a sudden decrease of H_2 values, in line with the results of [11,15] and with the reasoning of (R3). As this happens, and since the syngas LHV is partly influenced by H_2 production, the syngas LHV demonstrates this trend.

The predicted variation of tar content with increasing ER for both rubberwood and wood pellets is considered in Fig. 12. As mentioned earlier, increasing ER enhances T as a result of a higher input air within the gasifier. Consequently, a higher quality syngas is produced resulting in a reduction of the tar content. The increased T also facilitates tar cracking and thus the tar may decompose into lighter gases which may assist in increasing the combustible products in the syngas, ultimately decreasing the tar content [55,64].

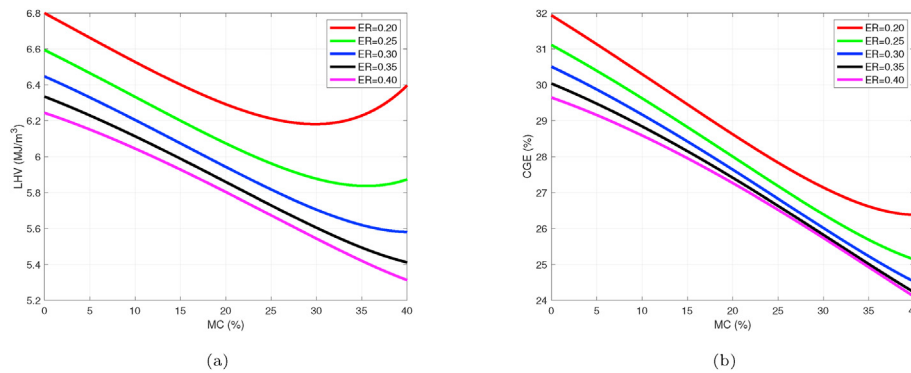


Fig. 11. Predicted variation for different ER values for (a) LHV_{gas} and (b) CGE, for rubberwood.

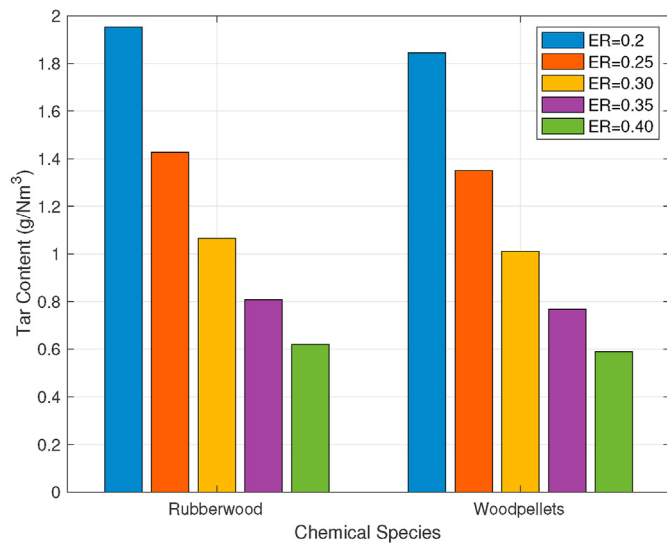


Fig. 12. Predicted variation of tar production for different values of ER for both rubberwood and wood pellet feedstocks (MC = 18.5%).

3.4. Minor gasification products

This section focuses on the minor gasification products encapsulated within the model, H₂S and NH₃. The purpose of including them is to estimate the concentrations of the primary sulphur-based and primary nitrogen-based contaminants within biomass gasification. Although some previous authors have considered the

production of H₂S [18], the production of NH₃ is novel in stoichiometric equilibrium modelling.

Fig. 13 show the variation in NH₃ and H₂S concentration for different ER values and increasing MC, respectively, for forest waste residue. Fig. 13a provides a comparison with the modelling results of [38] showing that, at an MC = 40%, there is extremely good agreement between the NH₃ and H₂S concentrations predicted by the model and those estimated by Ref. [38]. The NH₃ concentration is about 0.0122% for the model and approximately 0.015% for [38] at an ER = 0.1275 and displays a sharp decrease for both models as the ER increases towards 0.255. The H₂S concentration, however, is far less and remains almost constant with changes in ER as depicted, decreasing slightly with each ER increase. For increasing ER, T is enhanced and more of the biomass is transformed into syngas which in turn decreases the amount of volatiles, tar, char and contaminating gases such as NH₃ and H₂S. Also, note that H₂S is present in very small quantities in the output of the gasifier. This is because sulphur in feedstock is normally absent or contained in traces, which has prompted authors to neglect it as an output since its value does not contribute significantly to the main products of the gasifier. Fig. 13b shows the variation of NH₃ and H₂S concentrations with increasing MC, from which it is evident that the NH₃ concentration increases with increasing MC, while that of H₂S remains almost constant.

4. Conclusion

This paper provides a comprehensive equilibrium model for understanding the gasification process in a downdraft gasifier, incorporating a global reaction which includes all the gaseous

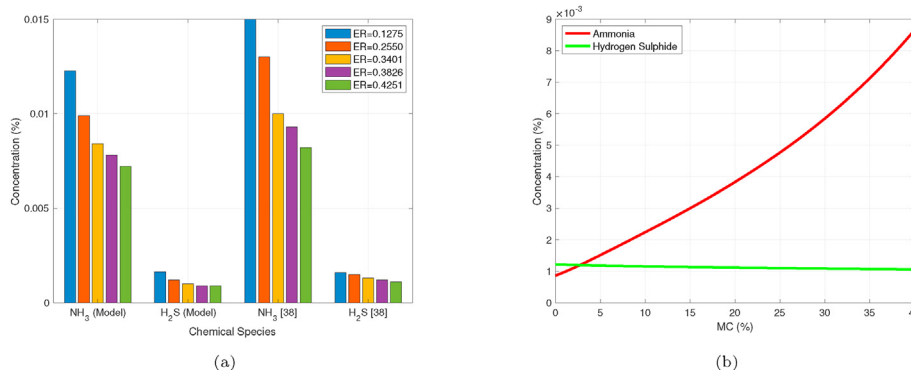


Fig. 13. Predicted variation in NH₃ and H₂S concentration for forest waste residue for (a) different ER values compared with the model results of [38] (MC = 40%) and (b) increasing MC (ER = 0.326).

species and the yields of tar and char, the latter of which is determined by implementing the boudouard reaction. In addition, the gasification temperature is determined via the solution of a fully coupled equation set resulting in a solver with improved convergence properties. To account for tar production in the model a new exponential best fit curve is generated, based on previous experimental data for tar creation in downdraft gasifiers, and the resulting correlation is implemented to account for the molar tar yield.

The syngas composition, gasification temperature, tar and char yields and the concentrations of the contamination gases predicted by the model shows very good agreement with experimentally obtained values and investigations and other recent comparable gasification models, suggesting that the current model can be reliably used to perform engineering simulations of downdraft gasification systems and undertake process design, evaluation and optimisation of gasification technology.

From the results obtained, the following conclusions are drawn:

1. The concentrations of H₂ and CO₂ increase with MC, while the CO concentration decreases. N₂ concentration remains constant while CH₄ concentration gradually increases with increasing MC.
2. T increases with ER and decreases with MC for gasification reasons mentioned in 3.1.2.
3. The tar yield decreases with increasing ER and MC due to a better quality syngas.
4. The boudouard reaction is a reliable approach for predicting char yield.
5. The LHV and CGE decrease with an increase in ER and T.
6. The concentration of NH₃ decreases with increasing ER values and increases with increasing MC, while the concentration of H₂S remains almost constant, decreasing slight with increasing ER and MC.
7. It is shown that equilibrium models are able to provide reliable predictions of syngas composition.

Funding

This research did not receive any specific grant from funding agencies in the public, commercial, or not-for-profit sectors.

Data availability

Datasets related to this article can be found at <https://data.mendeley.com/datasets/jtwtrbhfcb/3>, hosted at Mendeley Data [47].

CRedit authorship contribution statement

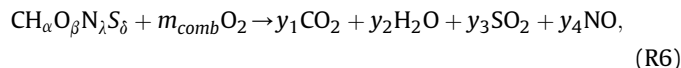
A. Ibrahim: Conceptualization, Methodology, Software, Validation, Formal analysis, Investigation, Data curation, Writing – original draft, Visualization. **S. Veremieiev:** Conceptualization, Methodology, Writing – review & editing. **P.H. Gaskell:** Conceptualization, Methodology, Writing – review & editing.

Declaration of competing interest

The authors declare that they have no known competing financial interests or personal relationships that could have appeared to influence the work reported in this paper.

Appendix A. Stoichiometric Combustion Reaction

The derivation of the ER equation [65,66] comes from the global reaction for combustion of biomass in oxygen and is defined in Section 2, where m_{gas} is the actual number of molecules of oxygen in the system. According to the global combustion reaction for a particular feedstock:



the stoichiometric balance of which consists of elemental mass balances for each of the following species C, H, O, N, S:

$$C : y_1 = 1, \tag{A.1}$$

$$H : y_2 = \frac{\alpha}{2}, \tag{A.2}$$

$$O : 2y_1 + y_2 + 2y_3 + y_4 = \beta + 2m_{comb}, \tag{A.3}$$

$$N : y_4 = \lambda, \tag{A.4}$$

$$S : y_3 = \delta. \tag{A.5}$$

By substituting Eqns. (A.1), (A.2), (A.4) and (A.5) into Eqn. (A.3), the following expression for m_{comb} is obtained:

$$m_{comb} = \left(1 + \frac{\alpha}{4} - \frac{\beta}{2} + \frac{\lambda}{2} + \delta \right). \tag{A.6}$$

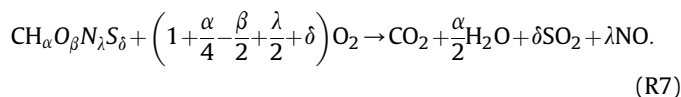
Next, using the definition of the ER:

$$ER = \frac{m_{gas}}{m_{comb}} = \frac{m_{gas}}{\left(1 + \frac{\alpha}{4} - \frac{\beta}{2} + \frac{\lambda}{2} + \delta \right)}, \tag{A.7}$$

and accordingly:

$$m_{gas} = \left(1 + \frac{\alpha}{4} - \frac{\beta}{2} + \frac{\lambda}{2} + \delta \right) \times ER. \tag{A.8}$$

Thus the combustion reaction simplifies as follows:



The biomass formation enthalpy is computed as a function of the molar LHV (J/mol) of the biomass [5,37,65], according to:

$$h_{f,bm}^{\circ} = LHV_{bm} + \sum_{i=1}^4 y_i h_{f,i}^{\circ}, \tag{A.9}$$

where $\sum_{i=1}^4$ is repeated over all products of complete combustion reaction (R6). The molar LHV can be calculated from the specific HHV (J/kg) of the biomass on a d.b. [5,37,65] as:

$$LHV_{bm} = HHV_{bmspec} \times M_{bm} - h_{vap} \left(\frac{\alpha}{2} \right), \tag{A.10}$$

where $\frac{\alpha}{2}$ is the number of moles of water produced per mole of biomass as per the combustion reaction (R7) and $h_{vap} = 44,000 J/mol$ is the enthalpy of vaporisation of water at standard temperature. The specific HHV_{bmspec} (MJ/kg) is calculated via an empirical correlation proposed by Channiwala and Parikh [67]: where y_{ASH} is the percentage weight of ash in biomass on a d.b. as reported in the proximate analysis of the feedstocks.

$$\text{HHV}_{\text{bmspec}} = 0.3491y_C + 1.1783y_H + 0.1005y_S - 0.1034y_O - 0.0151y_N - 0.0211y_{\text{ASH}} \quad (\text{A.11})$$

References

- [1] S. Sansaniwal, K. Pal, M. Rosen, S. Tyagi, Recent advances in the development of biomass gasification technology: a comprehensive review, *Renew. Sustain. Energy Rev.* 72 (2017) 363–384.
- [2] U. Kumar, M.C. Paul, CFD modelling of biomass gasification with a volatile break-up approach, *Chem. Eng. Sci.* 195 (2019) 413–422.
- [3] M. Puig-Arnavat, J.C. Bruno, A. Coronas, Review and analysis of biomass gasification models, *Renew. Sustain. Energy Rev.* 14 (9) (2010) 2841–2851.
- [4] A.M. Salem, M.C. Paul, An integrated kinetic model for downdraft gasifier based on a novel approach that optimises the reduction zone of gasifier, *Biomass Bioenergy* 109 (2018) 172–181.
- [5] M. La Villetta, M. Costa, N. Massarotti, Modelling approaches to biomass gasification: a review with emphasis on the stoichiometric method, *Renew. Sustain. Energy Rev.* 74 (2017) 71–88.
- [6] T. Dahou, F. Defoort, S. Thiéry, M. Grateau, M. Campargue, S. Bennici, M. Jeguirim, C. Dupont, The influence of char preparation and biomass type on char steam gasification kinetics, *Energies* 11 (8) (2018) 2126.
- [7] T. Dahou, F. Defoort, B. Khiari, M. Labaki, C. Dupont, M. Jeguirim, Role of inorganics on the biomass char gasification reactivity: a review involving reaction mechanisms and kinetics models, *Renew. Sustain. Energy Rev.* 135 (2021) 110136.
- [8] T. Dahou, F. Defoort, M. Jeguirim, C. Dupont, Towards understanding the role of k during biomass steam gasification, *Fuel* 282 (2020) 118806.
- [9] A. Tamosiūnas, A. Chouchène, P. Valatkevicius, D. Gimžauskaitė, M. Aikas, R. Uscila, M. Ghorbel, M. Jeguirim, The potential of thermal plasma gasification of olive pomace charcoal, *Energies* 10 (5) (2017) 710.
- [10] B. Khiari, M. Jeguirim, L. Limousy, S. Bennici, Biomass derived chars for energy applications, *Renew. Sustain. Energy Rev.* 108 (2019) 253–273.
- [11] Z. Zainal, R. Ali, C. Lean, K. Seetharamu, Prediction of performance of a downdraft gasifier using equilibrium modeling for different biomass materials, *Energy Convers. Manag.* 42 (12) (2001) 1499–1515.
- [12] A. Mountouris, E. Voutsas, D. Tassios, Solid waste plasma gasification: equilibrium model development and exergy analysis, *Energy Convers. Manag.* 47 (13–14) (2006) 1723–1737.
- [13] M.J. Prins, K.J. Ptasiński, F.J. Janssen, From coal to biomass gasification: comparison of thermodynamic efficiency, *Energy* 32 (7) (2007) 1248–1259.
- [14] A. Melgar, J.F. Pérez, H. Laget, A. Horillo, Thermochemical equilibrium modelling of a gasifying process, *Energy Convers. Manag.* 48 (1) (2007) 59–67.
- [15] A.K. Sharma, Equilibrium modeling of global reduction reactions for a downdraft (biomass) gasifier, *Energy Convers. Manag.* 49 (4) (2008) 832–842.
- [16] M. Puig-Arnavat, J.C. Bruno, A. Coronas, Modified thermodynamic equilibrium model for biomass gasification: a study of the influence of operating conditions, *Energy Fuels* 26 (2) (2012) 1385–1394.
- [17] S. Jarungthammachote, A. Dutta, Thermodynamic equilibrium model and second law analysis of a downdraft waste gasifier, *Energy* 32 (9) (2007) 1660–1669.
- [18] H.-J. Huang, S. Ramaswamy, Modeling biomass gasification using thermodynamic equilibrium approach, *Appl. Biochem. Biotechnol.* 154 (1–3) (2009) 14–25.
- [19] R. Karamarkovic, V. Karamarkovic, Energy and exergy analysis of biomass gasification at different temperatures, *Energy* 35 (2) (2010) 537–549.
- [20] V.B. Silva, A. Rouboa, Using a two-stage equilibrium model to simulate oxygen air enriched gasification of pine biomass residues, *Fuel Process. Technol.* 109 (2013) 111–117.
- [21] N.S. Barman, S. Ghosh, S. De, Gasification of biomass in a fixed bed downdraft gasifier—a realistic model including tar, *Bioresour. Technol.* 107 (2012) 505–511.
- [22] A.Z. Mendiburu, J.A. Carvalho Jr., C.J. Coronado, Thermochemical equilibrium modeling of biomass downdraft gasifier: stoichiometric models, *Energy* 66 (2014) 189–201.
- [23] A. Gagliano, F. Nocera, F. Patania, M. Bruno, D.G. Castaldo, A robust numerical model for characterizing the syngas composition in a downdraft gasification process, *Compt. Rendus Chem.* 19 (4) (2016) 441–449.
- [24] E.S. Aydin, O. Yucel, H. Sadikoglu, Development of a semi-empirical equilibrium model for downdraft gasification systems, *Energy* 130 (2017) 86–98.
- [25] M. Costa, N. Massarotti, G. Cappuccio, C. Chang, A. Shiue, C. Lin, Y. Wang, Modeling of syngas production from biomass energy resources available in taiwan, *Chem. Eng. Sci.* 37 (2014).
- [26] M. Costa, M. La Villetta, N. Massarotti, Optimal tuning of a thermo-chemical equilibrium model for downdraft biomass gasifiers, *Chem. Eng.* 43 (2015) 439–444.
- [27] A. Abuadala, I. Dincer, G. Naterer, Exergy analysis of hydrogen production from biomass gasification, *Int. J. Hydrogen Energy* 35 (10) (2010) 4981–4990.
- [28] J. Corella, J. Herguido, J. Gonzalez-Saiz, Steam gasification of biomass in fluidized bed-effect of the type of feedstock, in: *Pyrolysis and Gasification*, Elsevier Applied Science London, 1989, pp. 618–623.
- [29] E. Azzone, M. Morini, M. Pinelli, Development of an equilibrium model for the simulation of thermochemical gasification and application to agricultural residues, *Renew. Energy* 46 (2012) 248–254.
- [30] Y.-i. Lim, U.-D. Lee, Quasi-equilibrium thermodynamic model with empirical equations for air–steam biomass gasification in fluidized-beds, *Fuel Process. Technol.* 128 (2014) 199–210.
- [31] S. Rupesh, C. Muraleedharan, P. Arun, A comparative study on gaseous fuel generation capability of biomass materials by thermo-chemical gasification using stoichiometric quasi-steady-state model, *Int. J. Energy. Environ. Eng.* 6 (4) (2015) 375–384.
- [32] T. Yamazaki, H. Kozu, S. Yamagata, N. Murao, S. Ohta, S. Shiya, T. Ohba, Effect of superficial velocity on tar from downdraft gasification of biomass, *Energy Fuels* 19 (3) (2005) 1186–1191.
- [33] A.V. Bridgwater, Review of fast pyrolysis of biomass and product upgrading, *Biomass Bioenergy* 38 (2012) 68–94.
- [34] S. Ferreira, E. Monteiro, P. Brito, C. Vilarinho, A holistic review on biomass gasification modified equilibrium models, *Energies* 12 (1) (2019) 160.
- [35] A.K. Sharma, Modeling and simulation of a downdraft biomass gasifier 1. model development and validation, *Energy Convers. Manag.* 52 (2) (2011) 1386–1396.
- [36] H.P. Robert, W.G. Don, O.M. James, *Perry's Chemical Engineers' Handbook*, Nova lorque, 1984.
- [37] R.T. Balmer, *Modern Engineering Thermodynamics-Textbook with Tables Booklet*, Academic Press, 2011.
- [38] A. Gambarotta, M. Morini, A. Zubani, A non-stoichiometric equilibrium model for the simulation of the biomass gasification process, *Appl. Energy* 227 (2018) 119–127.
- [39] P. Basu, *Biomass Gasification and Pyrolysis: Practical Design and Theory*, Academic press, 2010.
- [40] F. Guo, Y. Dong, L. Dong, C. Guo, Effect of design and operating parameters on the gasification process of biomass in a downdraft fixed bed: an experimental study, *Int. J. Hydrogen Energy* 39 (11) (2014) 5625–5633.
- [41] N. Striugas, K. Zakarauskas, A. Dziugys, R. Navakas, R. Paulauskas, An evaluation of performance of automatically operated multi-fuel downdraft gasifier for energy production, *Appl. Therm. Eng.* 73 (1) (2014) 1151–1159.
- [42] M. Dogru, C. Howarth, G. Akay, B. Keskinler, A. Malik, Gasification of hazelnut shells in a downdraft gasifier, *Energy* 27 (5) (2002) 415–427.
- [43] M. Dogru, A. Midilli, C.R. Howarth, Gasification of sewage sludge using a throated downdraft gasifier and uncertainty analysis, *Fuel Process. Technol.* 75 (1) (2002) 55–82.
- [44] P. Lv, Z. Yuan, L. Ma, C. Wu, Y. Chen, J. Zhu, Hydrogen-rich gas production from biomass air and oxygen/steam gasification in a downdraft gasifier, *Renew. Energy* 32 (13) (2007) 2173–2185.
- [45] R. Wei, H. Li, Y. Chen, Y. Hu, H. Long, J. Li, C.C. Xu, *Environmental Issues Related to Bioenergy*, Comprehensive Renewable Energy, 2020.
- [46] V. Kirsanovs, A. Zandeckis, C. Rochas, et al., Biomass gasification thermodynamic model including tar and char, *Agron. Res.* 14 (2016) 1321–1331.
- [47] A. Ibrahim, S. Veremieiev, P. Gaskell, *Equilibrium Model Solver (ems) [online]* (2022), <https://doi.org/10.17632/jtwttrbhfcb.3>.
- [48] V. Maxim, C.-C. Cormos, A.-M. Cormos, S. Agachi, Mathematical modeling and simulation of gasification processes with carbon capture and storage (ccs) for energy vectors poly-generation, in: *Computer Aided Chemical Engineering*, vol. 28, 2010, pp. 697–702. Elsevier.
- [49] T. Jayah, L. Aye, R.J. Fuller, D. Stewart, Computer simulation of a downdraft wood gasifier for tea drying, *Biomass Bioenergy* 25 (4) (2003) 459–469.
- [50] M. Barrio, J. Hustad, M. Fossum, A small-scale stratified downdraft gasifier coupled to a gas engine for combined heat and power production, *Progress in thermochemical biomass conversion* (2001) 426–440.
- [51] S.J. Yoon, Y.-I. Son, Y.-K. Kim, J.-G. Lee, Gasification and power generation characteristics of rice husk and rice husk pellet using a downdraft fixed-bed gasifier, *Renew. Energy* 42 (2012) 163–167.
- [52] P. Dutta, V. Pandey, A. Das, S. Sen, D. Baruah, Down draft gasification modelling and experimentation of some indigenous biomass for thermal applications, *Energy Proc.* 54 (2014) 21–34, 0.
- [53] F. Patuzzi, D. Basso, S. Vakalis, D. Antolini, S. Piazzi, V. Benedetti, E. Cordioli, M. Baratieri, State-of-the-art of small-scale biomass gasification systems: an extensive and unique monitoring review, *Energy* 223 (2021) 120039.
- [54] V. Kirsanovs, D. Blumberga, I. Veidenbergs, C. Rochas, E. Vīgants, G. Vīgants, Experimental investigation of downdraft gasifier at various conditions, *Energy Proc.* 128 (2017) 332–338.
- [55] D.S. Upadhyay, A.K. Sakhiya, K. Panchal, A.H. Patel, R.N. Patel, Effect of equivalence ratio on the performance of the downdraft gasifier—an experimental and modelling approach, *Energy* 168 (2019) 833–846.
- [56] X. Li, J. Grace, C. Lim, A. Watkinson, H. Chen, J. Kim, Biomass gasification in a circulating fluidized bed, *Biomass Bioenergy* 26 (2) (2004) 171–193.

- [57] L. Damiani, A. Trucco, Biomass gasification modelling: an equilibrium model, modified to reproduce the operation of actual reactors, in: ASME Turbo Expo 2009: Power for Land, Sea, and Air, American Society of Mechanical Engineers Digital Collection, 2009, pp. 493–502.
- [58] M. Kumar, B. Paul, D.S. Yadav, Effect of moisture content and equivalence ratio on the gasification process for different biomass fuel, *Int. J. Mech. Eng. Technol.* 7 (6) (2016).
- [59] R.F. Naryanto, H. Enomoto, A. Vo Cong, K. Fukadu, Z. Zong, M.K. Delimayanti, C. Chunti, R. Noda, The effect of moisture content on the tar characteristic of wood pellet feedstock in a downdraft gasifier, *Appl. Sci.* 10 (8) (2020) 2760.
- [60] E. Shayan, V. Zare, I. Mirzaei, Hydrogen production from biomass gasification; a theoretical comparison of using different gasification agents, *Energy Convers. Manag.* 159 (2018) 30–41.
- [61] Z. Yao, S. You, T. Ge, C.-H. Wang, Biomass gasification for syngas and biochar co-production: energy application and economic evaluation, *Appl. Energy* 209 (2018) 43–55.
- [62] M.-H. Cho, T.-Y. Mun, J.-S. Kim, Air gasification of mixed plastic wastes using calcined dolomite and activated carbon in a two-stage gasifier to reduce tar, *Energy* 53 (2013) 299–305.
- [63] R. Xiao, B. Jin, H. Zhou, Z. Zhong, M. Zhang, Air gasification of polypropylene plastic waste in fluidized bed gasifier, *Energy Convers. Manag.* 48 (3) (2007) 778–786.
- [64] S. Salaudeen, P. Arku, A. Dutta, Gasification of plastic solid waste and competitive technologies, in: *Plastics to Energy*, Elsevier, 2019, pp. 269–293.
- [65] M.L. de Souza-Santos, *Solid Fuels Combustion and Gasification: Modeling, Simulation*, CRC Press, 2010.
- [66] J. Ancheyta, *Modeling of Processes and Reactors for Upgrading of Heavy Petroleum*, CRC Press, 2013.
- [67] S. Channiwala, P. Parikh, A unified correlation for estimating h_hv of solid, liquid and gaseous fuels, *Fuel* 81 (8) (2002) 1051–1063.

Nomenclature

Upper case letters

C_p : Molar heat capacity, (J/molK)

G : Total Gibbs free energy, (J/mol)
 H : Total enthalpy, (J/mol)
 M : Molecular mass of species, (kg/mol)
 N_{tot} : Number of moles of raw gas at temperature
 T : per 1 mol of biomass, (mol)
 N_{gas} : Number of moles of dry gas at temperature
 T_0 : per 1 mol of biomass, (mol)
 R : Universal gas constant, (J/molK)
 T : Gasification temperature, (K)
 T_0 : Standard temperature, (K)
 V_m : Molar volume of ideal gas at temperature
 T_0 : and pressure p_0 , (m³/mol)

Lower case letters

g : Gibbs free energy, (J/mol)
 g_f : Gibbs free energy of formation (J/mol)
 h : Enthalpy, (J/mol)
 h_f : Formation enthalpy of species (J/mol)
 K : Equilibrium constant
 m : Number of moles of air per 1 mol of biomass (mol)
 p : Partial pressure (Pa)
 p_0 : Standard pressure (Pa)
 s : Entropy, (J/mol)
 s_f : Entropy of formation (J/molK)
 w : Number of moles of water per 1 mol of biomass (mol)
 x : Number of moles, (mol)

Greek letters

α : Number of atoms of hydrogen in the biomass feedstock
 β : Number of atoms of oxygen in the biomass feedstock
 λ : Number of atoms of nitrogen in the biomass feedstock
 δ : Number of atoms of sulphur in the biomass feedstock
 ν : stoichiometric number of moles, (mol)